Chapter II

Lagrangian General Circulation Based on the Time-scale of Particle Motion

Seiji SUGATA
National Institute for Environmental Studies

Abstract

A new method to analyze particle motion in the general circulation in a Lagrangian sense is proposed. The method counts the flux of a particle through a surface by considering Lagrangian information of the particle, namely, duration of the particle's location on each side of the surface. Transit which is sandwiched between locations longer than a standard duration on both sides of the surface is selected as an effective flux. Analysis of motions of a large number of particles by the new method with some different standard durations can abstract a Lagrangian global circulation from motions of a large number of particles in the troposphere and lower stratosphere in a general circulation obtained by the Center for Climate System Research / National Institute for Environmental Studies atmospheric general circulation model. The existence of barriers to transport in both mid-latitudes is quantitatively shown. Zonally averaged meridional circulation obtained by the method shows one cell circulation in the troposphere, which has the same characteristics as the structure obtained by the transformed Eulerian mean method. The time-scale of atmospheric motions causing global meridional Lagrangian transport is also discussed.

1 Introduction

Atmospheric general circulation causes global transport of materials through the atmosphere. Investigation of the general circulation from the Lagrangian viewpoint, in addition to the Eulerian viewpoint, is neccesary to understand how the distribution of materials in the atmosphere is controlled by the circulation. If we could follow an infinitely large number of air parcels for a long time and describe all motions of the parcels, we would be able to perfectly understand the Lagrangian general circulation. However, since it is impossible for us to explore an infinitely large number of Lagrangian motions, we need schemes to statistically describe the Lagrangian general circulation. This study develops such a scheme and a description of the Lagrangian general circulation follows this new scheme.

In the Lagrangian sense, the whole atmosphere can be considered as being divided into different mixing regions. A mixing region is defined as some region of space within which the distribution of an inhomogeneous tracer becomes essentially homogeneous over some time scale (mixing time) and which is bounded by (almost) impermeable barriers to transport (Pierrehumbert and Yang 1993). In the largest view, the troposphere, the stratosphere, and the upper atmospheric regions are individual mixing regions.

If we consider a Lagrangian view of general circulation, we are usually interested not in transport or in diffusion within the mixing region but in transport through the barrier between the two adjacent mixing regions.

Many types of analysis have been developed to investigate the Lagrangian view of the general circulation. A meridional circulation averaged zonally in a Eulerian sense was one of the starting points for understanding of global Lagrangian circulation. The meridional circulation consists of 3 cells in the troposphere and 2 cells in the stratosphere. However, a meridional circulation deduced from observation of a distribution of materials, such as ozone, consists of 1 cell in the troposphere and 1 cell in the global stratosphere. Thus the circulation obtained by the usual Eulerian approach is inconsistent with the Lagrangian circulation. This discrepancy between the Eulerian zonal mean meridional circulation and the Lagrangian zonal mean meridional circulation is mainly attributed to the existence of large scale waves, such as baroclinic waves in the troposphere and Rossby waves in the stratosphere (Matsuno 1980). In these waves, air parcels ascend at higher latitudes and descend at lower latitudes on elliptic trajectories whose major axes are nearly horizontal. Overlapping of these parcels' motions produces what is known as the indirect circulation at mid-latitudes in the Eulerian meridional circulation.

A residual circulation in the Transformed Eulerian Mean method is obtained

by a sophisticated Eulerian approach. The residual circulation abstracts the Lagrangian circulation to an extent, since the circulation is obtained by subtracting an indirect circulation caused by the waves mentioned above from a Eulerian zonally averaged meridional circulation. However, it must be noted that the circulation was arrived at from a Eulerian viewpoint, and whether the meridional circulation makes an accurate abstract of the Lagrangian circulation or not should be supported by direct approaches of Lagrangian parcel statistics (c.g., Kida 1977, 1983).

Another way to abstract the Lagrangian circulation is to consider the Lagrangian motions of parcel groups and to regard the motions as a combination of movements of representative points of the group and some kind of diffusion from that point. The Generalized Lagrangian mean (GLM) method selects a center of mass of parcel groups at a representative point. Meridional circulation obtained by the GLM shows strong convergence, which is one of defeats of the GLM. This convergence arises for the following reason: The time required for air particles to exchange between 2 mixing regions through a barrier is much longer than that required for them to diffuse within each mixing region. Therefore, GLM flow is affected by the diffusion within each mixing region to which the parcels belongs, and tends to converge to the center of each mixing region. A global Lagrangian transport, that is transport between mixing regions, is hidden by the convergence.

Kida (1983) calculated trajectories of a large number of air parcels in a quasi-equilibrium general circulation obtained by a general circulation model (GCM). He considered that movement of the center of mass could be divided into an irreversible component caused by diffusion and a reversible component caused by true advection. He proposed a method adding a forward and a backward Lagrangian mean analysis to remove the irreversible component, that is the convergence of the center of mass. However, this modified GLM methods does not seem to be appropriate to analyze Lagrangian circulation in the troposphere, where circulation is very complicated.

There are some other methods to distribute Lagrangian particle motion among an advective component and a diffusive component. Plumb and Mahlman (1987) considered an effective transport of the zonally-averaged budget equation of the mixing ratio of a quasi-conserved constituent. They distribute an antisymmetric part in the flux-gradient parameterization of the eddy flux to an effective Lagrangian advection. Zonally averaged circulation obtained by this method is a 2-cell Hadley-like structure in the troposphere and a single cell in the stratosphere. Their scheme also has the shortcoming that it is not a direct approach to the Lagrangian circulation.

Most of the schemes reviewed above have been motivated to describe wave

- mean flow interaction or to construct a 2-D chemical transport model. A new approach of Lagrangian parcel statistics using direct Lagrangian information of a large number of particles should be developed. This new scheme would be a direct utilization of trajectories of a large number of parcels and would be suitable to estimate long term Lagrangian transport between mixing regions.

In Section 2, a new approach to count the flux of a particle through an arbitrary surface is proposed. The scheme considers the duration of a particle's presence on each side of the surface and abstracts an effective flux to contribute global transport of long-lived materials from all the fluxes. The new method is applied to the motion of a large number of particles in a general circulation obtained by an integration of a GCM. The motion is obtained by integration of a chasing model developed for this study. Descriptions of the GCM, the tracer model, and the process of seeking trajectories are mentioned in Section 3. The trajectories obtained in Section 3 is analyzed by the flux method. The results are described in Section 4.

2 Description of a New Method

Motions in the atmosphere cover a wide range of spatial and temporal scales. However, not all of the scales of motion contribute much to global tracer transport. A new method which abstracts the movements of particles which are effective in a global tracer transport from motions of a large number of particles is proposed in this section. Consider a meridional redistribution of material transported by the atmospheric general circulation. If a parcel of air including the material is transported meridionally from a certain latitude by the atmospheric motion and then returns meridionally to the initial latitude again within a time shorter than both the life-time of the material and the diffusive time-scale with the surrounding air, the meridional movement of the parcel does not contribute much to the meridional redistribution of the material except for the change due to weak diffusion. Meridional movements in the atmosphere, therefore, can be divided into effective movements, those which contribute substantially to the global material circulation and have longer time-scales, and ineffective movements, those which do not contribute substantially to the circulation and have shorter time-scales. Thus, consideration of the time-scales of the motions transporting materials is very important for estimation of a general Lagrangian circulation. As mentioned in the introduction, my interest is focused on large-scale and long-term transport between mixing-regions in the atmosphere from a Lagrangian viewpoint. Therefore a new method using some kinds of low-pass filters to abstract the Lagrangian motion from the atmospheric circulation is necessary.

One new method of measuring the flux of particles uses Lagrangian information about the particles motion. Consider a particle whose trajectory is obtained in the general circulation in a Lagrangian sense. We focus on the number of intersections of a particle into a certain surface during a certain period. We assume a certain standard time-scale T, which should be determined according to what time-scale we are investigating in the Lagrangian circulation. The essence of this new method of assessing flux is to neglect intersections whose periods are shorter than T because such short time-scale oscillating movement does not contribute to global transport on time-scales longer than T. A successive T time location on one side of the surface is adopted as a standard to judge the effectiveness of intersections to the surface for global transport. An intersection is only selected as an effective transit when the particle concerned has experienced, successively, a T time stay on one side of the surface before the intersection and the particle will experience, successively, a T time stay on the other side immediately after the intersection. In other words, the particle will be located on one side immediately after the selected transit for T successive time and the preceding T successive time stay of the particle occurred on the other side. Thus the definition of the transit selected by the time-scale T is introduced with definitions of its time and location relative to the surface.

We will discuss meridional Lagrangian transport using this new method. The method is applied to a large number of particles transported in an atmospheric general circulation obtained by a general circulation model in this study. Surfaces of equal latitude will be taken as the surfaces used in this method. Since motions carried by baroclinic waves, which induce indirect cells in an Eulerian sense, in mid-latitudes, have a time-scale from a few days to a week, time, T, should be adopted as the time-scale for this approach. Thus the time-scales from $T = 0$ days to $T = 2$ weeks will be considered. Fluxes obtained by the new scheme with $T = 0$ are the same as those in the usual Eulerian flux, as can be seen by the definition of the method.

3 Description of Models

An off-line tracer model, which uses stored data for wind and cumulus mass flux obtained by integrations of an atmospheric general circulation model (CCSR/NIES AGCM), is developed. The general circulation model, the transport model, and the numerical procedure used are described in this section.

3.1 Description of GCM

The Center for Climate System Research / National Institute for Environmental Studies atmospheric general circulation model (CCSR/NIES AGCM) was used to obtain general circulation data for trajectory integration by a tracer model in this study. The model is transformed spectrally in the horizontal direction and differentiated in the vertical direction on a sigma coordinate. The physical parameterization includes a sophisticated radiation scheme with a cloud water scheme, a turbulence closure scheme with cloud effects, orographic gravity wave drag, and a simple land-surface submodel. Further description of the CCSR/NIES AGCM is presented in another chapter in this monograph.

The resolution for the CCSR/NIES AGCM in this study was T42L20. Baroclinic waves are resolved on this resolution and it is expected that the statistical nature of Lagrangian general circulation is reproduced on this resolution.

After a preliminary integration for 4 years, the GCM was integrated for 1 year to obtain data for the tracer model. Horizontal velocities u, v, vertical velocity $d\sigma/dt$, temperature T, surface pressure Ps, and vertical mass flux by cumulus convection F_c were stored as 4 hour averaged 4 hour interval data. The vertical velocity and the vertical mass flux are defined at staggered levels from the σ levels at which the other data are defined. The vertical velocity is rectified by a compensating downward flux according to the cumulus mass flux to facilitate in the tracer model described in the next subsection.

The monthly mean data in February obtained by integration of the GCM (Figs 1 and 2) are compared with results in section 4.

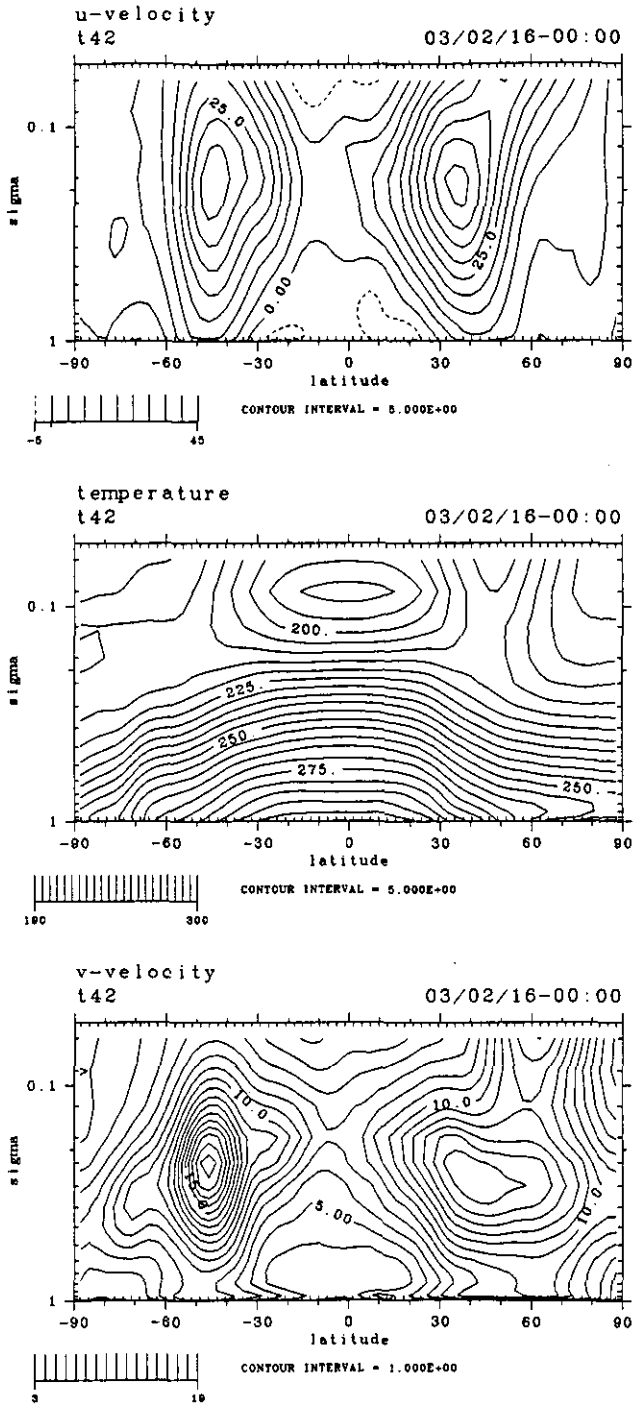

Figure 1: Meridional section of zonal mean zonal wind (a), temperature (b), and variance of meridional velocity from zonal mean (c) obtained by the CCSR/NIES GCM for February. Contour interval is 5m/s (a), 5K (b), and 1m/s(c), respectively.

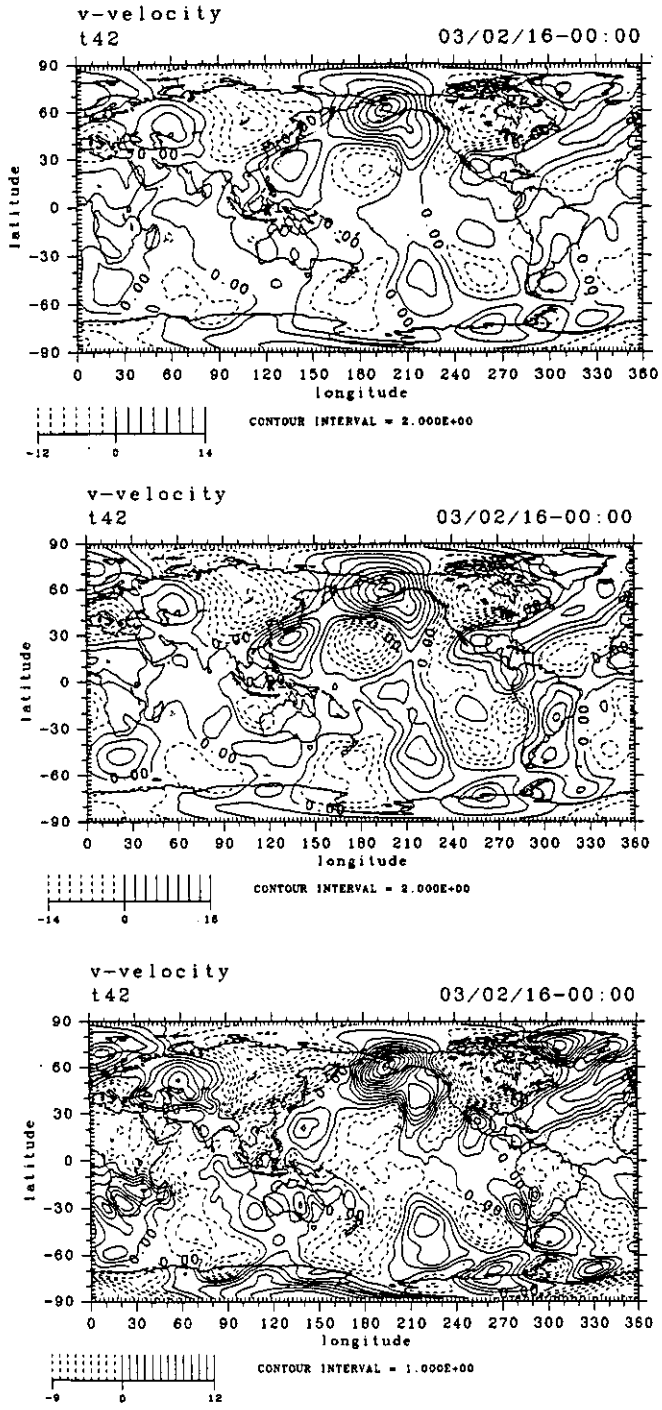

Figure 2: Horizontal distribution of horizontal wind for February from GCM. Horizontal wind averaged for whole layers (a) and meridional winds averaged for the upper layer above 500 hPa (b) and for the lower layer below 500 hPa (c), respectively. Contour intervals are 2 m/s (a), 2 m/s (b), and 1 m/s (c), respectively.

3.2 Tracer Model for Particle Trajectory Calculation

An off-line tracer model is developed in this study to investigate trajectories of a large number of idealized particles which follow the atmospheric motions exactly. The tracer model uses stored data of wind, temperature, surface pressure, and vertical mass flux by cumulus convection, which were obtained by integration of the GCM described above. In the transport model, each particle is advected by atmospheric motion or convected by cumulus convection in each calculation time step. In each calculation time step, a judgment is first made as to whether a given particle is captured by cumulus convection; then the particles captured are convected to upper layers, and the particles not captured are advected. A procedure of transport by the cumulus convection will be described below. The following kinetic relationship is used to calculate advection:

$$d\boldsymbol{x}/dt = \boldsymbol{v}(\boldsymbol{x}, t), \tag{1}$$

where v is velocity at a location $\boldsymbol{x}$ and the time t, is integrated by a fourth order Runge-Kutta-Gill method using 4 hour average winds. A sigma coordinate σ is used in the vertical direction and $d\sigma/dt$ is used as vertical velocity. The vertical velocity is rectified by a compensating downward flux in the grid point where a cumulus mass flux exists. The velocity field v is linearly interpolated both in the horizontal and vertical directions from 8 neighboring grids.

Cumulus convection exerts a great influence on global atmospheric transport since tracers are vertically diffused by convection. The CCSR/NIES AGCM uses a simplified Arakawa-Schubert scheme as its cumulus parameterization. This scheme considers cumulus spectra and upward cumulus mass flux, cloud base level, cloud top level, downdraft mass flux, and so on. Cumulus spectra are not distinguished in the present tracer model. Only the total cumulus mass flux integrated through all spectra is used in the tracer model. Compensating downward flux is considered at a place without cumulus convection, as mentioned in the previous subsection. However, downdraft flux is not considered in the tracer model since that flux is a smaller and occurs over a shorter transport distance than those of the upward cumulus mass flux.

When a particle is in a layer with a cumulus convection mass flux, whether a particle is captured by that cumulus convection or not depends on the sign of convergence of the cumulus mass flux, which is in the layer concerned. Consider a k-th layer which contains the air mass M per unit horizontal area and which has an upward mass flux, $F_c(k-1)$, at its lower boundary and the flux, $F_c(k)$, at its upper boundary, both per unit horizontal area. If the layer has a non-zero convergence, namely $F_c(k-1) - F_c(k) > 0$, then the probability of any particle being captured by the cumulus convection is given by the ratio of the amount of mass converged in

the layer during 1 calculation time step to the total mass contained in the layer:

$$\frac{(F_c(k-1)-F_c(k))\Delta t}{M}, \tag{2}$$

where Δt is the time step of the calculation. A particle which is not captured by such convection is advected as calculated by Eqn. (1). The particle captured by the convection is transported upward by it and released in the higher layer. The layer where the particle will be released is determined as follows: (a) the particle is lifted up to the next higher layer, the l-th layer. (b) If there is a positive divergence of the cumulus mass flux in that layer, namely $F_c(l)-F_c(l-1)>0$, then probability of the particle being released in that layer is given by the ratio of decrease in upward cumulus mass flux at the layer to the upward mass flux at the bottom of the layer:

$$\frac{F_c(l)-F_c(l-1)}{F_c(l-1)}. \tag{3}$$

(c) If the particle is not released at that layer, then the procedure is repeated from step (a) with the next higher layer, $l=l+1$. When the particle is released, its new horizontal position is the same as that before convection and its new vertical position is randomly chosen in the layer of release.

Particles are initially located globally on 89 latitude circles from 88.0° north to 88.0° south at 2.0 degree intervals and in 18 vertical levels from $\sigma=0.95$ to 0.10 at 0.05 intervals. In the longitudinal direction particles are located within equal longitudinal intervals on the circles in each latitude and height. The number of particles in a longitudinal direction is 360 × cos(latitude(in radians)). This latitudinal dependence means that the number of particles is proportional to the length of the latitude circle and that each particle represents an air mass almost equal to those represented by all other particles. Total numbers of particles for 1 and all 18 levels are 20,626 and 371,268, respectively. Each particle represents approximately 1.2×10^{13} Kg from February data for the global mean surface pressure and the number of particles. Hereafter the flux of particles will be presented in terms of mass fluxes. The range of the particles extends from the whole of the troposphere to the lower stratosphere.

Two tracer calculations whose starting times are different from each other were done: 1 for for winter from January to March and the other for summer from July to September. All results which will be shown in this paper are for the former one. The time step of the trajectory calculation was 30 minutes. The particles' positions, namely latitude, longitude, σ, and pressure, were saved every 4 hours. On the basis of the position data, the new method introduced in the previous section was applied to every transit of a particle through surfaces of equal latitude for February and August. The surfaces concerned are those from Lat. 82°30″N through Lat. 82°30″S at 5° intervals.

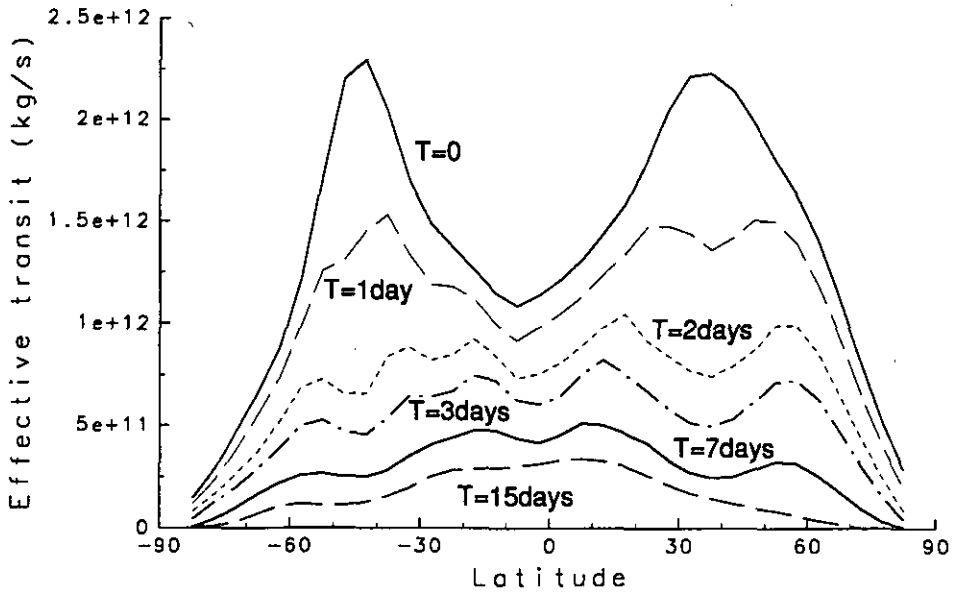

Figure 3: Meridional distribution of meridional mass flux calculated by the scheme introduced in this paper (see text for details) for several time-scale of qualification. Northward and southward fluxes are summed and vertically integrated on each latitude. Unit is Kg/s.

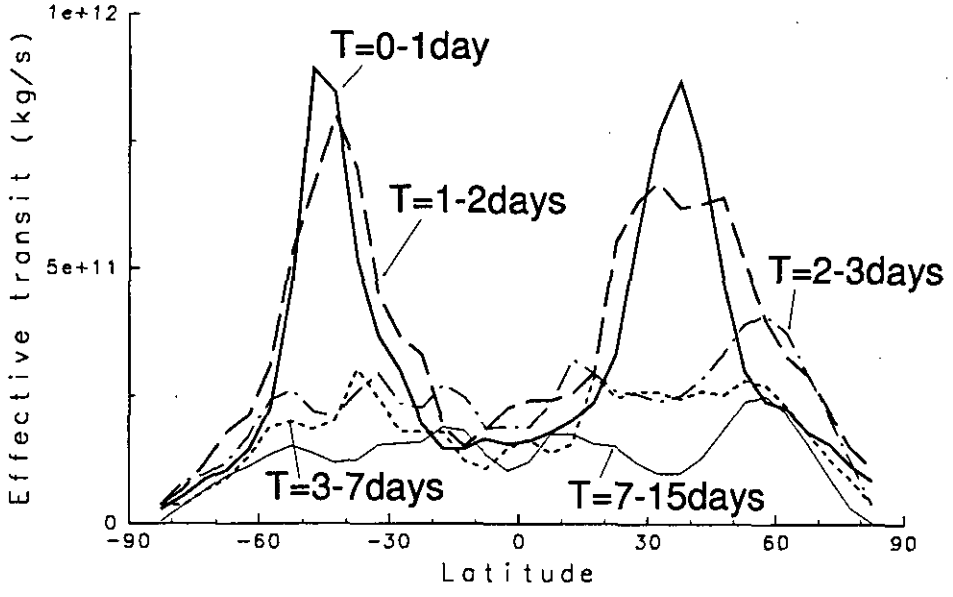

Figure 4: Meridional distribution of meridional mass flux obtained by the new scheme for several time-scale ranges obtained by subtracting values of fluxes among time-scales in Fig. 3. For example, a distribution of $T = 1 - 2$ days is the subtraction of $T = 2$ days from $T = 1$ day in Fig. 3.

4 Results

Figure 3 shows the latitudinal distributions of mass flux as the sum of northward and southward fluxes through each latitude counted by the scheme as defined in section 3 for several T-times. The line with $T = 0$, which corresponds to the usual flux in a Eulerian = sense, shows 2 maximums at both mid-latitudes and a local minimum near the equator. The maximums represent predominance of baroclinic waves in the mid-latitudes, where particles are frequently oscillated meridionally by movements induced by cyclonic and anticyclonic waves. The minimum near the equator corresponds to the ITCZ, which is the boundary between 2 Hadley cells in both hemispheres, and constitutes a potential barrier to material transport across it. A similar meridional distribution to that with $T = 0$ is apparent in the line with $T = 1$ days, although there is a small dip in the northern mid-latitudes. As the time used in the flux analysis increases to longer than 2 days, a meridional distribution comes to show a different structure compared to that with $T = 0$ days. On lines with $T = 2, 3$, and 7 days, local minimums are evident at both mid-latitudes, where maximums had been shown with $T = 0$ days, although a minimum near the equator still remains. There are basically 4 maximums and 3 minimums on the lines, and the minimums in the mid-latitudes come to show relatively smaller values compared to the minimum near the equator. Although there is a local minimum near Lat. 30°S in addition to that at Lat. 45°S in the lines with $T = 2$ and 3 days, the minimum near Lat. 30°S disappears in the line with $T = 7$ days. The local minimums at the mid-latitudes are not well-defined with $T = 15$ days.

The mass flux for $T = 0 - 1$ day is a subtraction of the flux with $T = 1$ day from that with $T = 0$ days (Fig. 4). Since a mass flux obtained with any given period T days under Lagrangian conditions means the flux carried by atmospheric motions with time-scales of more than T days, the flux of $T = 0 - 1$ represents the mass flux carried by atmospheric motions with time-scales of less than 1 day. Other fluxes shown in Fig. 4 are also mass fluxes carried by motions of each respective time-scale range. Much larger fluxes are shown by lines with $T = 0 - 1$ and $T = 1 - 2$ days at both mid-latitudes than those with other time-scales, which reveals that much of the mass transport occurring at mid-latitudes is carried by motions with time-scales shorter than 2 days. In other words, most of the mass transported northward (southward) through the mid-latitudes returns southward (northward) to the original side of the latitude within 2 days. Local minimums are shown by distributions of $T = 3 - 7$ and $T = 7 - 15$ days in the mid-latitudes, which suggests the existence of potential barriers to global material transport at the mid-latitudes on time-scales from a few days to a few weeks (Pierrehumbert and

Yang 1993) in addition to that at the ITCZ at lower latitudes. On the other hand, a minimum near the equator appears in analyses conducted at every time-scale range, which means that meridional transport is suppressed near the equator over both short and long time-scales. It is also noteworthy that the meridional position of the minimum near the equator moves northward as the time-scale increases (see Figs. 3 and 4).

Latitude-height sections of the total mass flux for $T = 0$ days has a peaks in each mid-latitude in the middle troposphere (Fig. 5 a). These 2 peak regions correspond to those where baroclinic waves are active (see Fig. 1 c). The flux selected for $T = 2$ days has hollow regions relative to that calculated for $T = 0$ days (see Figure 5 b) in the upper stratosphere through the lower stratosphere at the mid-latitudes compared to fig. 5 (a). Two local meridional minimums at each constant altitude, except for altitudes in the lower stratosphere, are present at both mid-latitudes. The vertical levels where mass flux is maximum at both mid-latitudes are closer to the surface relative to those calculated for $T = 0$ days. These trends show that the higher latitudes are separated from the lower latitudes at altitudes from the middle troposphere through lower stratosphere. In the lower troposphere there are four 4 in the meridional direction; 2 are at lower latitudes in both hemispheres and the other 2 are in mid-latitudes. The large mass fluxes for time-scale between 2 and 7 days are distributed in height from the middle of the troposphere to the lower troposphere at the mid-latitudes (Fig. 5 e). These regions correspond clearly to the regions of vigorous baroclinic waves activity (see Fig. 1) We can conclude from these fluxes for time-scales of 0 and 2 days and the difference between them (see Fig. 5 a, b, and e) that the predominant meridional motion at mid-latitudes accompanied by baroclinic waves has a time-scale of less than 2 days and that little effective transport through the mid-latitudes with a time-scale longer than 2 days is induced by the baroclinic waves. The flux for $T = 7$ days (see Fig. 5 c) shows that the meridional motions are confined close to the surface on this time-scale, particularly at mid-latitudes.

Mass fluxes on time-scales between 2 and 7 days have been evaluated by taking the difference between those calculated for 2 days and those calculated for 7 days (Fig. 5 f) The fluxes at these these 3 time-scales, 2, 7, and 2 to 7 days (see Fig. 5 b,c, and f, respectively) make it clear that the activities in the mid- and high- latitudes at a time-scale of 2 days do not result in much effective transport over any time-scale longer than 7 days.

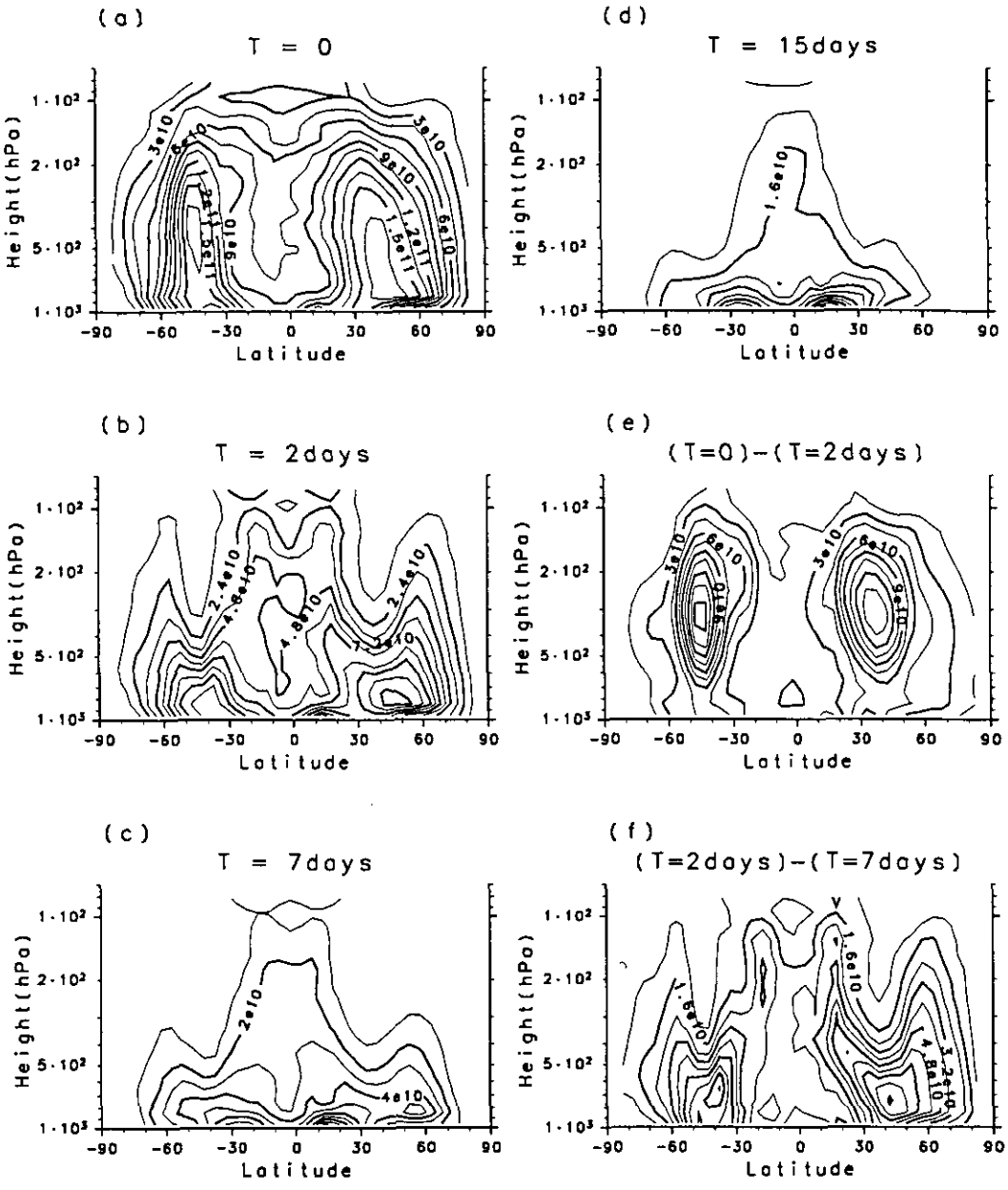

Figure 5: Meridional sections of total mass fluxes of a sum of northward and southward fluxes, which was selected by the new method. (a) - (d) are obtained for time-scale criteria with $T = 0, 2, 7$, and 15 days, respectively. (e) and (f) are for time-scale ranges with $0 - 2$ days and $2 - 7$ days, respectively, which are obtained by subtracting fluxes among (a), (b), and (c).

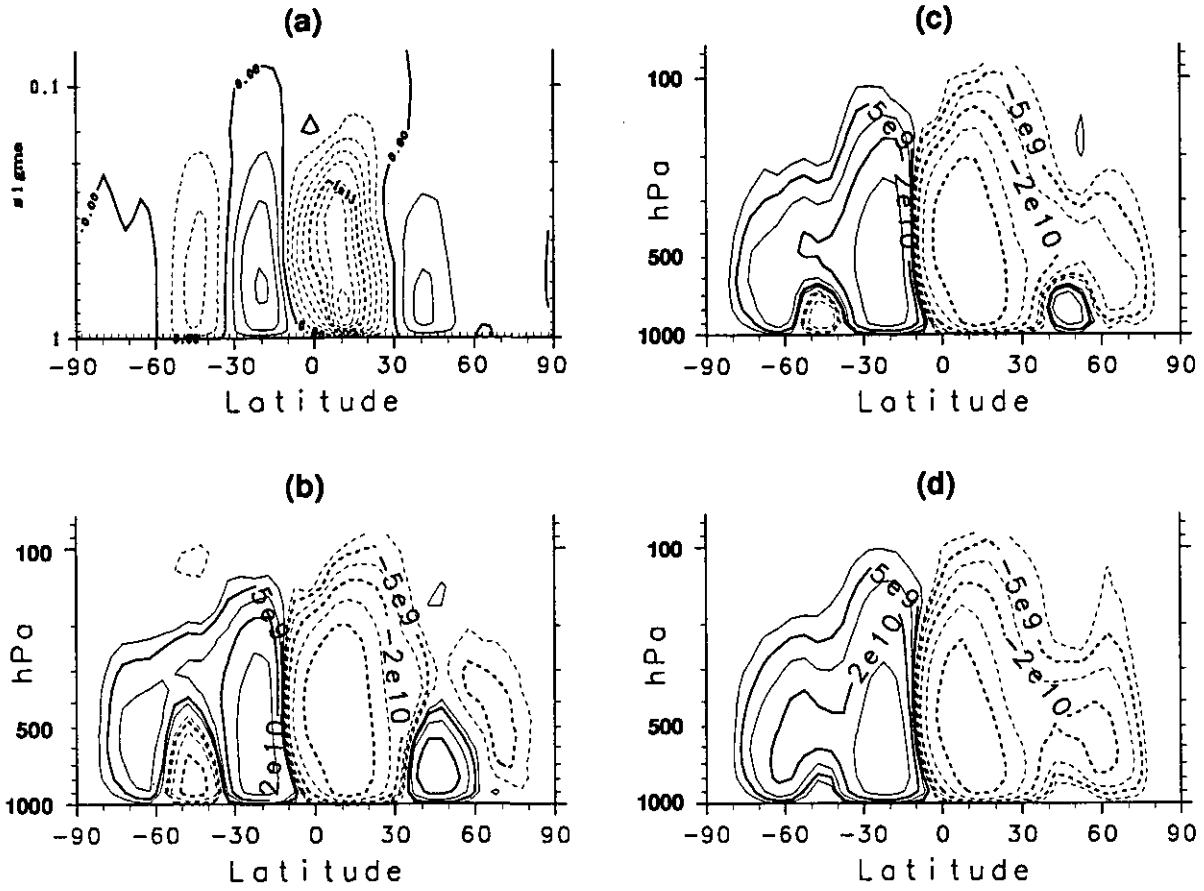

Figure 6: Meridional sections of stream functions for February. A stream function obtained from meridional velocity data and density data from the GCM (a). Stream functions obtained from meridional mass flux selected with time-scales of $T = 0, 2$, and 7 days (b, c, and d), respectively.

Though the mass flux described above is the sum of the northward and southward fluxes, net meridional flux was also calculated (Fig. 6 a). The Eulerian meridional mean circulation obtained from meridional velocity and density data from the CCSR/NIES AGCM mentioned in section 3 is typical in that it consists of 3 cells in each hemisphere. Although the stream function obtained from meridional mass flux obtained by the present scheme with $T = 0$ days (see Fig. 6 b) should have the same structure as that derived from the Eulerian data (see Fig. 6 a) since the variables coincide, there is a noticeable difference in the size of Ferrel cells between the data sets. The Ferrel cells from the Lagrangian calculation with $T = 0$ days were weaker and confined to lower levels relative to those evaluated with the Eulerian data. This difference due to the particle location data having been at 4 hour intervals and the position having been calculated from 4-hour averages of this 4-hour interval data. Namely, much of the transport induced by motions with time-scales shorter than 4 hours are omitted from the flux calculated even

in the $T = 0$ days analysis, and the difference between the $T = 0$ and $T = 2$ days analyses corresponds to the fluxes with time-scales shorter than 4 hours. As the time-scale used in the Lagrangian analysis increases, the Ferrel cells at mid-latitudes decrease and are restricted to close to the surface. From the data for 7 days, mid-latitude Ferrel cells disappear and a single cell structure occurs in each hemisphere (see Fig. 6 d). It should be noted that the contours for stream functions in mid-latitudes descend locally from above the upper atmosphere and ascend from near the surface. It is well known that a similar structure apparent in contours of stream functions obtained by the Transformed Eulerian Mean method.

The horizontal distributions of both the northward and southward fluxes (Fig. 7 a) have 2 maximums in the longitudinal direction from around Lat. 50° N through Lat. 60° N. The shapes of these horizontal flux distributions constitute a wavy structure with a wave-number of 2, the characteristics of which are apparent also in a plot of the net northward flux alone (Fig. 7 b). These fluxes look like pipelines for the exchange of materials between the high and middle latitudes.

The meridional direction of the fluxes at the lower latitudes are approximately opposite those at higher latitudes with a border around Lat. 40° (N and S) dividing them. Although the clear wavy structure is not apparent at the lower latitudes, 3 or 4 pairs of northward and southward fluxes in a longitudinal direction exist there. The structures at lower latitudes are clearer when observed from different vertical heights, and therefore they will be discussed below. The resemblance between structures of the horizontal distributions of mass flux (Figs. 7 a and b) indicates that the position where the northward flux begins is definitely separated from that where the southward flux originates. Comparing the plot of the northward and southward fluxes separately with a plot of the net northward flux (see Fig. 7 a and b) to horizontal sections of meridional velocity averaged in February in a usual Eulerian sense (see Fig. 2), the meridional directions of fluxes selected by time-scales of 7 days in a Lagrangian sense depend rather on the directions of meridional velocity averaged monthly in the usual Eulerian sense.

Since analysis of the vertical dependence of the horizontal distribution of mass transport (not shown) reveals that the dependence is not very large, particularly at higher latitudes, this dependence was investigated for the upper (Fig. 8) and lower (Fig. 9) halves of the atmosphere, with pressures less that and greater than about 550 hPa. Mass transport in the upper half of the atmosphere at low latitudes was more active than that at higher latitudes. Pairs of fluxes of opposite direction with borders near the equator appeared. While there are upper parts of so-called Hadley cells, pairs in the mid-Pacific and mid-Atlantic Oceans show an indirect circulation unlike typical Hadley cells. With borders in the regions between Lat.. 30° – 40° N and S, the meridional directions at fluxes at higher latitudes were opposite

those at lower latitudes; also the strengths of those at higher latitudes were much weaker than those at lower latitudes. In the lower half of the atmosphere, the fluxes at northern mid-latitudes were comparable to those at low latitudes (Fig. 9). Southward fluxes extend meridionally from high latitudes to near the equator in East Asia, and a northward flux extends from Central America to Northern Europe. In a global Lagrangian sense, these fluxes are pipelines connecting the high latitudes with the low latitudes. The shapes of pairs of fluxes in the lower half of the atmosphere at low latitudes are not as clear as those in the upper layers. The meridional distributions of fluxes in the upper half of the atmosphere were opposite in direction from those in the lower half except for those from the mid-Pacific Ocean to Central America in the northern hemisphere (see Figs. 8 a, b and 9 a, b).

Horizontal distributions of total fluxes of northward and southward fluxes were investigated in the case of $T = 7$ days (Figs. 7 – 9 c). The total fluxes are indexes for the strength of potential barriers for transport. Total less fluxes which are drawn in blue (least) and green (less) in the figures are shown in both mid-latitude around Lat. 50° N and S and near the equator, where the distribution in the longitudinal direction is localized to a few positions at each latitude (Fig. 7 c). These regional little fluxes are potential barriers that are investigated in Fig. 3 as zonal mean small fluxes. In the upper layer (Fig. 8 c), there is no meridional minimum near the equator while both mid-latitudes are meridional minimums at all longitudes. The minimums in the mid-latitudes correspond to so called tropospheric jet stream. On the other hand, low latitudes show minimums while mid-latitudes do not show noticeable minimums except Tibetan highland. The effect of the Tibetan highland is shown (Fig. 7 c).

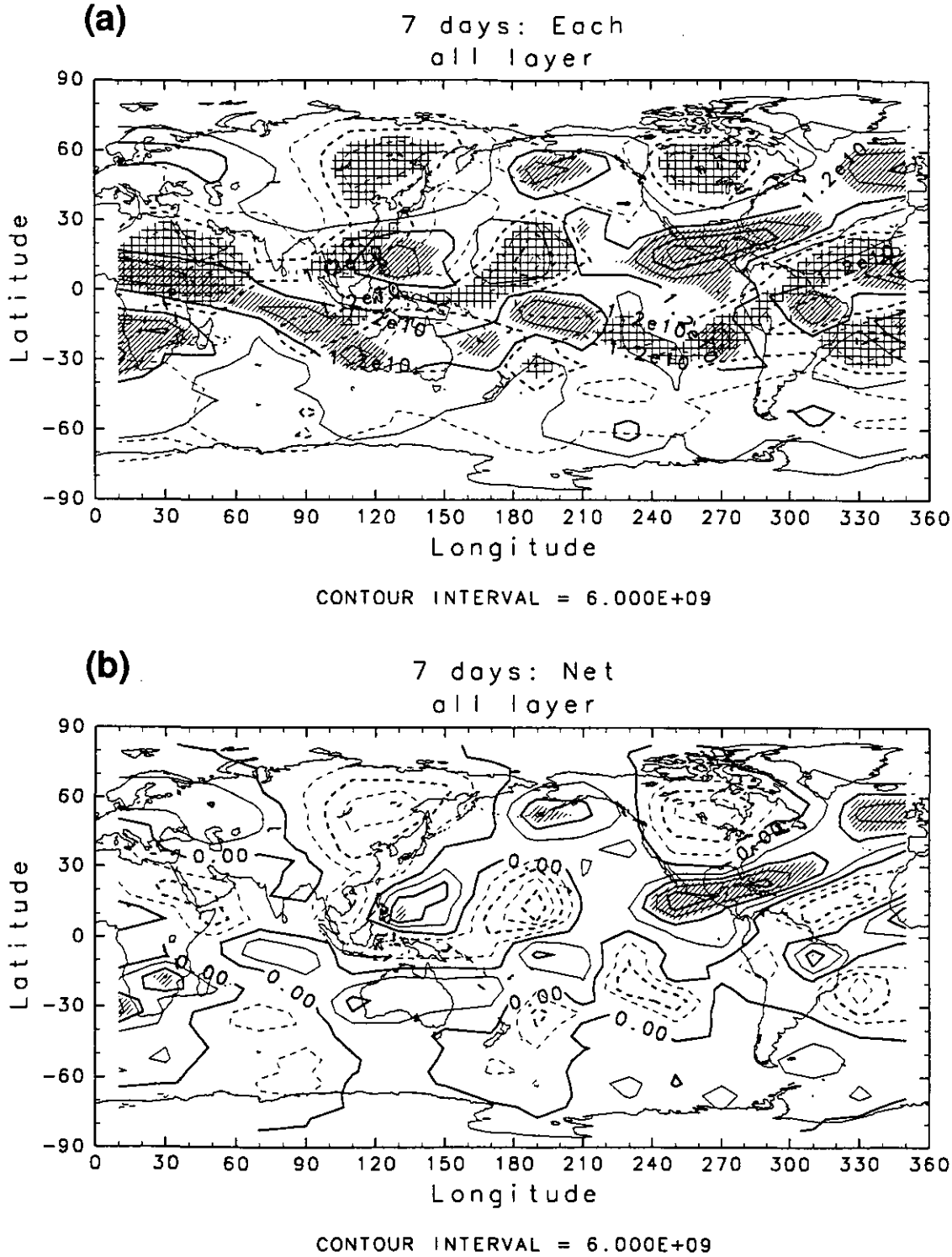

Figure 7: Horizontal distribution of mass flux selected by $T = 7$ days integrated through all heights. (a) Both northward flux and southward flux separately (b) net northward flux, and (c) sum of amounts of northward and southward fluxes. contours are drawn by solid line for northward flux and by broken line for southward flux in (a) and (b)

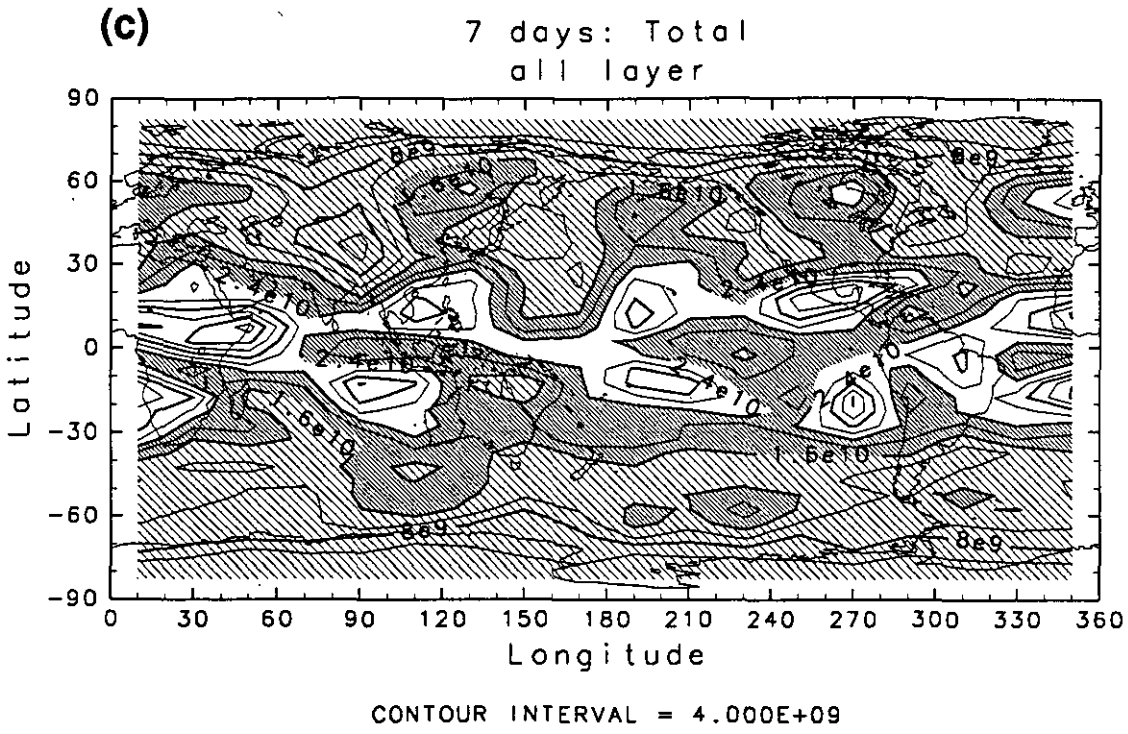

Figure 7: continued

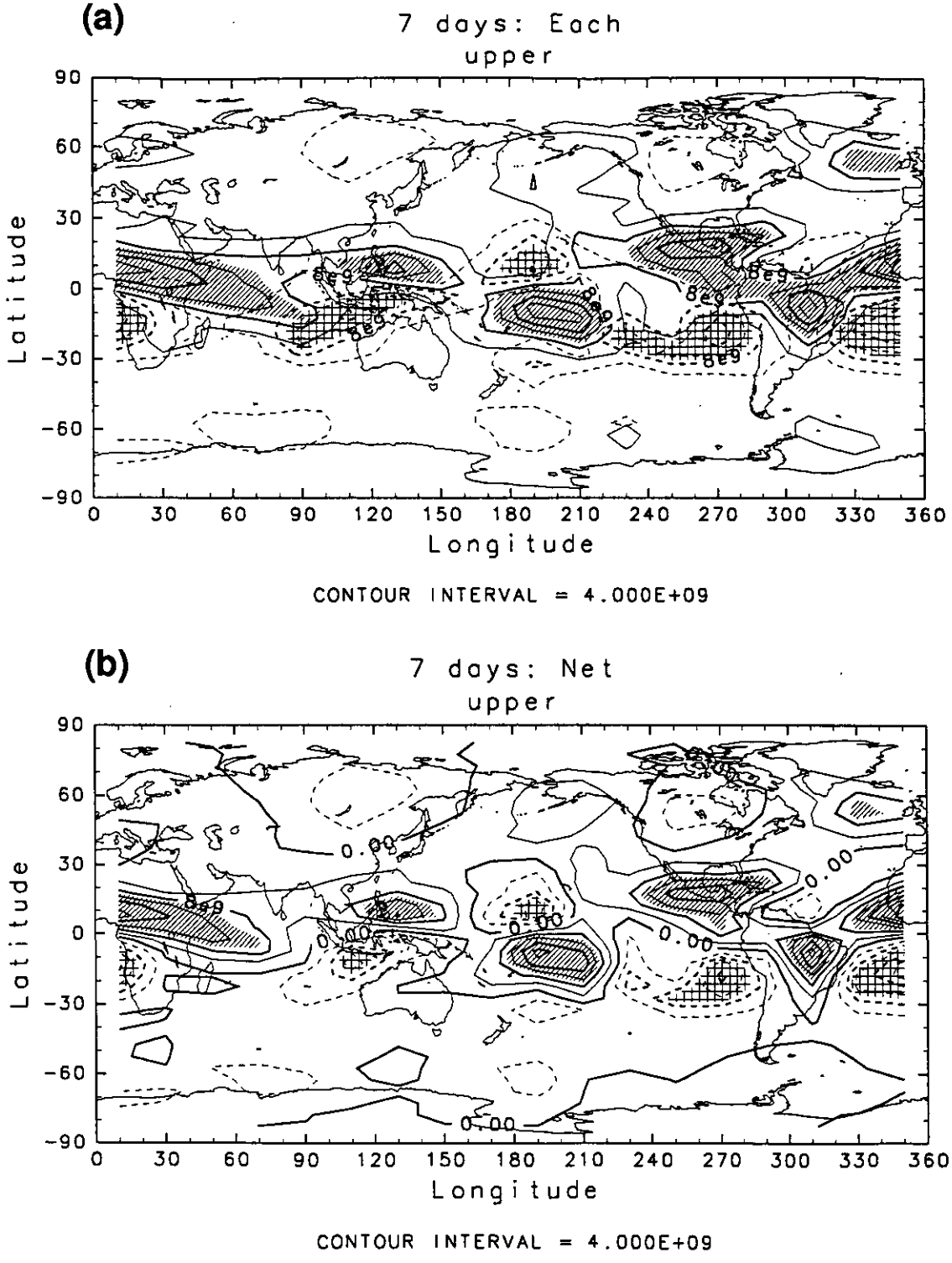

Figure 8: As in Fig. 7, except for integration above 550 hPa.

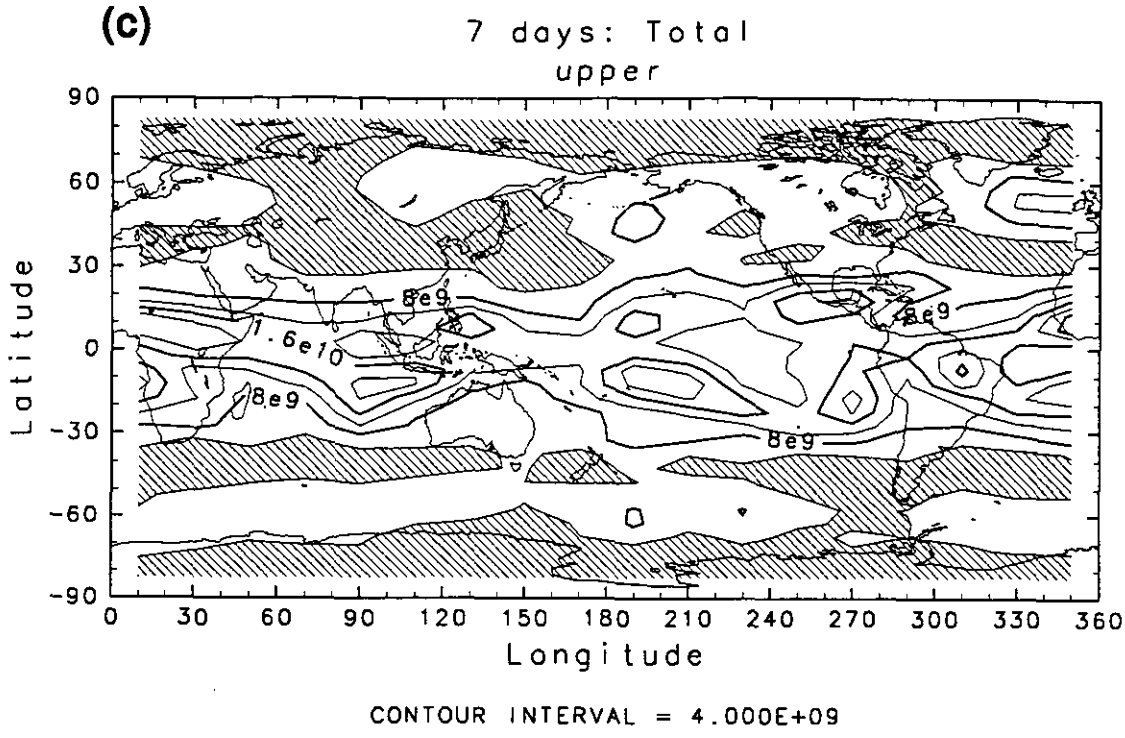

Figure 8: continued

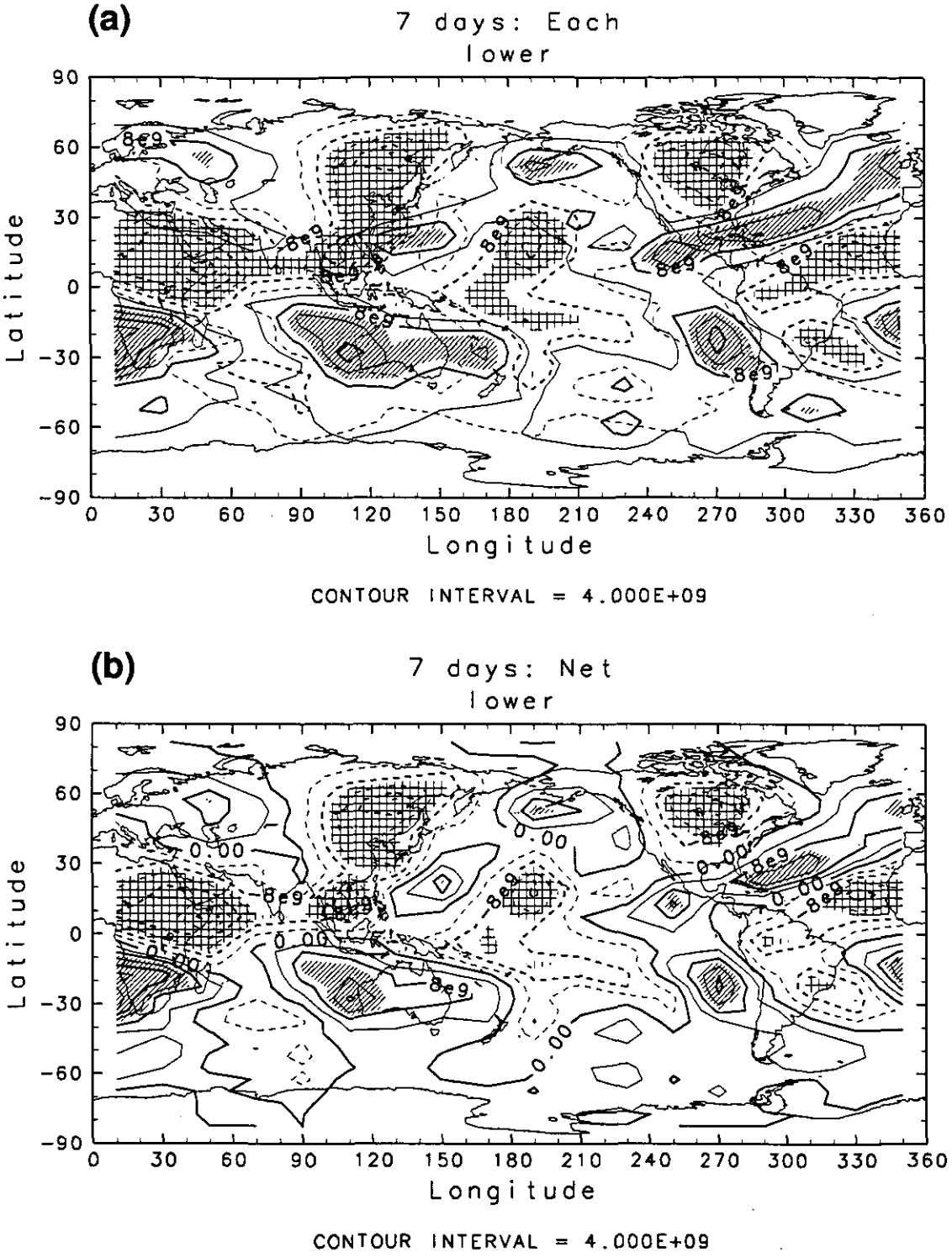

Figure 9: As in Fig. 7, except for integration below 550 hPa.

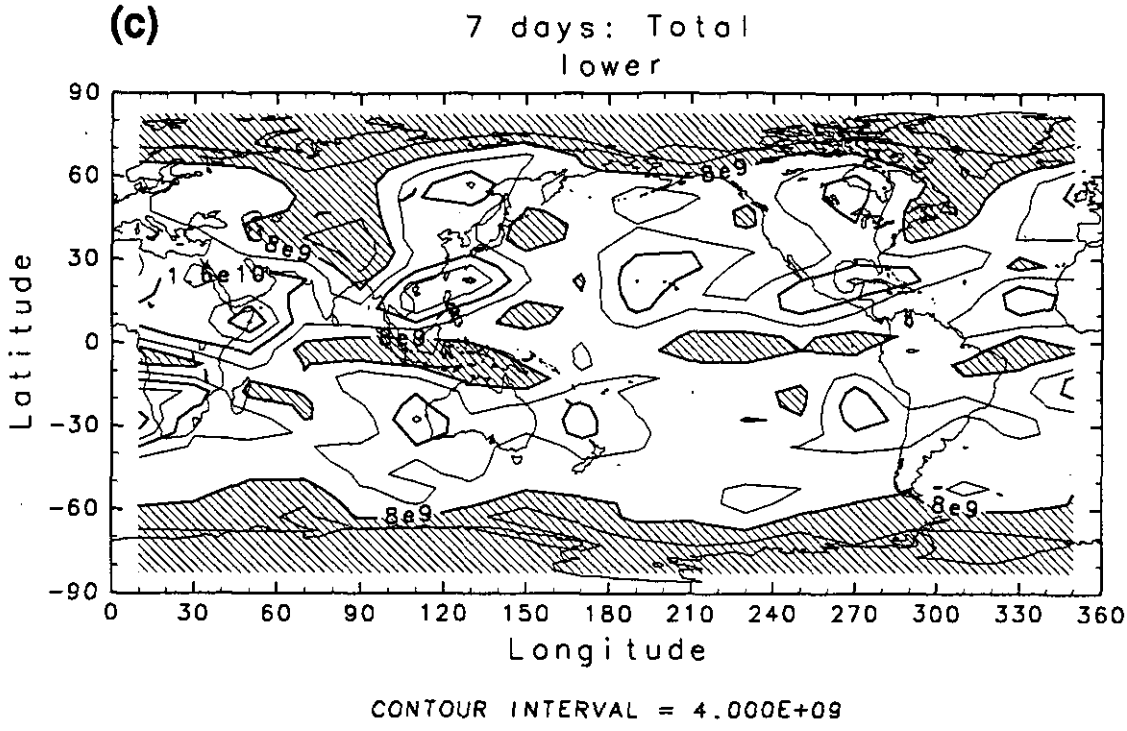

Figure 9: continued

5 Discussion

The tracer model developed in this study uses 4-hour average 4-hour interval data of a GCM and stored positions of particles during these 4-hour intervals. Therefore, atmospheric motions with time-scales shorter than 4 hours were omitted, even in the analysis for a time-scale of $T = 0$ days, as was mentioned i n the preceding section. The difference between the flux calculated by the GCM and that calculated by the Lagrangian approach presented here for $T = 0$ days (see Figs. 6 a and b) reveals that such short time-scale motions account for a significant fraction of the motions at mid-latitudes. Further studies using shorter interval data are necessary to investigate contributions of such short time-scale motions to global transport. However this result is similar one obtained with the usual Eulerian approach.

Potential barriers to global material transport in the troposphere exist in both the mid-latitudes at around Lat. 40° – 50° N and S and near the ITCZ. Near the ITCZ, the lower convergence zones contribute to the barrier of the ITCZ(see Fig. 9 d). On the other hand, the middle and upper troposphere, where baroclinic waves are vigorous, play the role of barrier in the mid-latitudes.

Sommeria et al. (1989) investigated a transport of dyes across strong jet streams in an annulus fluid in the laboratory; they showed that there is remarkably

little transport across the jet for very long periods of time. Pierrehumbert and Yang(1993) studied mixing on the isentropic surface and showed that the mid-latitudes play the role of a potential barrier for transport. These investigation of waves or jet streams as potential barriers done in these simpler flows have shown the existence of potential barriers at mid-latitude. The results obtained in this study reveal that such potential barriers do exist in the real atmosphere.

The dependence of meridional distributions of total mass flux northward and southward revealed processes at that the latitudes corresponding to the ITCZ play the role of a potential barrier for transport at all time-scales. On the other hand, processes at mid-latitudes work as potential barriers only over time-scales longer than a few days. In other words, the ITCZ is a potential barrier in both a Eulerian sense and a Lagrangian sense. On the other hand, processes at mid-latitudes are not barriers in a Eulerian sense, though they are barriers in a Lagrangian sense.

6 Conclusions

A new scheme is proposed for analyzing the flux of a particle whose trajectory is given through a surface. The scheme uses Lagrangian trajectory information. A time-scale T of the motion we want to describe is assumed and a successive time T location is defined as an effective location used as a standard for the selection of an effective transit. A transit through a surface is selected as the effective transit contributing to global transport when it is the most resent transit sandwiched temporally between 2 "effective locations" existing on opposite sides of the surface. The scheme acts as a kind of low-pass filter to the trajectory and discriminates between transits which are effective for global material transport and those which are not.

The scheme is applied to motions of a large number of particles in a general circulation obtained from the CCSR/NIES AGCM. Four hour averaged interval data of velocities, surface pressure, temperature, and upward mass flux of cumulus convection were stored by integration of the GCM for 1 year. Trajectories of a large number of particles were calculated by a tracer model developed for this study. The tracer model considers advection and convection of the particles. The upward convection due to cumulus convection is suitably handled by using the stored data of cumulus mass flux data from the GCM. Trajectories of nearly four hundred-thousands particles were calculated for 3 months from January to March. The scheme of flux described above is applied for trajectories of the particles for one month of February for surfaces of equal latitudes. The flux obtained by the scheme shows the existence of potential barriers to global material meridional transport in mid-latitudes in addition to that near the ITCZ. Although oscillating meridional

movements with short time-scales are dominant in the mid-latitudes due to active baroclinic waves, longer time-scale movements are suppressed in these regions. Clearly, the longitudinal positions where meridional transport is suppressed are localized in the longitudinal direction.

Acknowledgments

The author thanks Dr. Richard Weisburd for his help in improving English expressions.

References

Numaguti, A., M. Takahashi, T. Nakajima, and A. Sumi, 1995: Description of CCSR/ NIES Atmospheric General Circulation Model to be submitted to J. Mereor. Soc. Japan

Kida H. 1977: A numerical investigation of the atmospheric general circulation and stratospheric-tropospheric mass exchange: II. Lagrangian motion of the atmosphere. J.M.S.J Vol.55 71–70

Kida H. 1983: General circulation of air parcels and transport characteristics derived ¿from a hemispheric GCM: Part 2. Very long-term motions of air parcels in the troposphere and stratosphere. J.M.S.J Vol.61 510–523

Matsuno T. 1980: Lagrangian Motion of Air Parcels in the Stratosphere in the Presence of Planerary waves. Pageoph. Vol.118 189–216

Plumb R. A. and J. D. Mahlman, 1987: The Zonally averaged transport characteristics of the GFDL general circulation/transport model. J. Atmos. Sci. Vol.44 298–327

Pierrehumbert R. T. and H. Yang, 1993: Global chaotic mixing on isentropic surfaces. J. Atmos. Sci. Vol. 50 2462–2480

Sommeira, J., S. D. Meyers, and H. L. Swinney, 1988: Laboratory model of a planetary eastward jet. Nature, 337, 58-61